



**RELATIVE POSITION COVARIANCE  
ESTIMATION OF RESIDENT SPACE  
OBJECTS USING EXTRAPOLATED SINGLE  
PROPAGATION TECHNIQUE**

by  
**ARDRA SURESH**

**Under the Supervision of Dr. Sanat K Biswas**

**DEPARTMENT OF ELECTRONICS AND  
COMMUNICATION ENGINEERING**

---

**INDRAPRASTHA INSTITUTE OF INFORMATION  
TECHNOLOGY DELHI**

**JULY 2022**

**INDRAPRASTHA INSTITUTE OF  
INFORMATION TECHNOLOGY DELHI**



**RELATIVE POSITION COVARIANCE  
ESTIMATION OF RESIDENT SPACE  
OBJECTS USING EXTRAPOLATED SINGLE  
PROPAGATION TECHNIQUE**

by

**Ardra Suresh  
MT20143**

Submitted

in partial fulfillment of the requirements of the degree Master of Technology

to

INDRAPRASTHA INSTITUTE OF INFORMATION  
TECHNOLOGY DELHI

JULY 2022

## Certificate

This is to certify that the thesis titled "**RELATIVE POSITION COVARIANCE ESTIMATION OF RESIDENT SPACE OBJECTS USING EXTRAPOLATED SINGLE PROPAGATION TECHNIQUE**" being submitted by **Ardra Suresh** to the Indraprastha Institute of Information Technology Delhi, for the award of the Master of Technology, is an original research work carried out by her under my supervision. In my opinion, the thesis has reached the standards fulfilling the requirements of the regulations relating to the degree.

The results contained in this thesis have not been submitted in any part or full to any other university or institute for the award of any degree/diploma.

Dr.Sanat K. Biswas  
(Thesis Supervisor)

Department of Electronics and Communication Engineering  
Indraprastha Institute of Information Technology Delhi  
New Delhi 110020

July, 2022

*Dedicated to my parents  
Suresh HK and Jalaja TP*



# *Acknowledgements*

First and foremost, I extend my deep gratitude and appreciation to my supervisor Dr.Sanat K.Biswas, who inspired me and created a craving interest in this project. From the bottom of my heart, I express my gratitude for his sincere and excellent guidance, insightful comments, constructive criticism and friendly approach.

I cannot fully express in words my appreciation to all the faculty members of Indraprastha Institute of Information Technology, Delhi for the scholarly classes and for the direction and constant inspiration during the last two years. The knowledge they transferred, equipped me in this effort. I feel fortunate and is truly appreciative for being positively influenced by you.

I am really indebted to my parents, teachers and friends who provided every support in my work and for the help extended. Words are insufficient to convey my gratitude for the precious time you spent, your efforts and your guidance. Without your advice and unconditional dedication, I would not have been able to conceive and develop this project. Thank you all for the constant inspiration and encouragement.

# *Abstract*

Due to the ever-increasing space activities, there has been a stark increase in the number of space objects and debris, which include defunct satellites, pieces of space hardware, and launch vehicle remains. This poses a huge threat of collision to every space mission planned and for existing active satellites. It is crucial to have awareness about any possible conjunction event of active satellites with other resident space objects(RSO) so that a fatal collision can be avoided. Estimating the covariance associated with the relative position of the satellite and the RSO in the most accurate and computationally efficient way is the first step toward this. A new way to estimate this covariance using the ESPT Method by utilising TLE data of the space objects is discussed here. In this work, the ESPT Method, Monte Carlo method and Covariance Propagation Method is implemented and the effectiveness of the ESPT method is evaluated and compared with the conventional Monte Carlo approach and the Covariance Propagation method based on their utility and computation time.

# Contents

Certificate

Acknowledgements

Abstract

Contents

List of Figures

List of Tables

Abbreviations

<b>1</b>	<b>Introduction</b>	<b>1</b>
1.1	Goals and Objectives . . . . .	2
1.2	Motivation . . . . .	3
1.3	Dissertation Layout . . . . .	4
<b>2</b>	<b>Literature Review</b>	<b>5</b>
2.1	Space situational awareness . . . . .	5
2.2	Tracking of space objects . . . . .	6
2.3	Orbit Propagation . . . . .	8
2.3.1	Perturbations in Orbit . . . . .	9
2.4	Conjunction Events . . . . .	10
2.4.1	CLAPS Tool for conjunction analysis . . . . .	13
2.5	Collision Probability . . . . .	15
<b>3</b>	<b>Methodology</b>	<b>19</b>
3.1	Initial Implementation steps . . . . .	20

3.2	Filtering of irrelevant objects . . . . .	20
3.2.1	Date based Filter . . . . .	21
3.2.2	Apogee-perigee Filter . . . . .	21
3.3	Orbit Propagation . . . . .	21
3.3.1	Adding Perturbations while propagating . . . . .	22
3.4	Estimating with better accuracy . . . . .	23
3.4.1	Orbit Sampling . . . . .	24
3.4.2	Estimating the accurate TLE . . . . .	24
3.5	Covariance Matrix Estimation . . . . .	25
3.5.1	Monte Carlo Method . . . . .	26
3.5.2	Extrapolated Single Propagation Method . . . . .	27
3.5.3	Covariance Matrix Propagation Method . . . . .	30
<b>4</b>	<b>Results</b>	<b>33</b>
4.1	3D orbit visualisation . . . . .	33
4.2	Inter-satellite distance . . . . .	34
4.2.1	General Plots of ISD with time . . . . .	34
4.2.2	Box Plots of ISD with time . . . . .	36
4.3	Orbit Propagation visualisation . . . . .	37
4.4	Samples Plot . . . . .	38
4.4.1	ESPT Samples . . . . .	38
4.4.2	Monte Carlo Samples . . . . .	41
4.5	Mean and Standard Deviation Plots . . . . .	42
4.6	Comparison of Execution Time . . . . .	47
<b>5</b>	<b>Conclusion and Future Work</b>	<b>49</b>
5.1	Summary . . . . .	49
5.2	Scope for Future Work . . . . .	50
	<b>Bibliography</b>	<b>51</b>

# List of Figures

3.1	Block diagram depicting flow of implementation . . . . .	25
4.1	3D orbit of the object with NORAD CAT ID 43939 . . . . .	34
4.2	Inter-satellite distance with perturbations plot 1 . . . . .	35
4.3	Inter-satellite distance with perturbations plot 2 . . . . .	35
4.4	Box plot of inter-satellite distance in ESPT method . . . . .	36
4.5	Box plot of inter-satellite distance in MC method . . . . .	37
4.6	Samples Propagation - ESPT Method . . . . .	37
4.7	Samples Propagation - Monte Carlo Method . . . . .	38
4.8	ESPT samples at timestamp = 1s, 901s, 1801s, 2701s. . . . .	39
4.9	ESPT samples at timestamp = 3601s, 4501s, 5401s, 6301s. . . . .	40
4.10	MC samples at timestamp = 1s, 901s, 1801s, 2701s. . . . .	41
4.11	MC samples at timestamp = 3601s, 4501s, 5401s, 6301s. . . . .	42
4.12	Plot of Mean of Inter-satellite distance in X axis . . . . .	43
4.13	Plot of Mean of Inter-satellite distance in Y axis . . . . .	43
4.14	Plot of Mean of Inter-satellite distance in Z axis . . . . .	43
4.15	Plot of Standard deviation of ISD in X . . . . .	44
4.16	Plot of Standard deviation of ISD in Y . . . . .	44
4.17	Plot of Standard deviation of ISD in Z . . . . .	45
4.18	Plot of Standard deviation of ISD in X from covariance matrix . . . . .	45
4.19	Plot of Standard deviation of ISD in Y from covariance matrix . . . . .	45
4.20	Plot of Standard deviation of ISD in Z from covariance matrix . . . . .	46



# List of Tables

4.1 Comparison of Execution Times of all methods . . . . .	47
--	----



# Abbreviations

<b>TLE</b>	<b>Two Line Element-set</b>
<b>RSO</b>	<b>Resident Space Object</b>
<b>CDM</b>	<b>Conjunction Data Message</b>
<b>ASAT</b>	<b>Anti SATellite</b>
<b>MC</b>	<b>Monte Carlo</b>
<b>ESPT</b>	<b>Extrapolated Single Propagation Technique</b>
<b>LEO</b>	<b>Lower Earth Orbit</b>
<b>MEO</b>	<b>Medium Earth Orbit</b>
<b>GEO</b>	<b>Geosynchronous Earth Orbit</b>
<b>CAM</b>	<b>Collision Avoidance Manoeuvres</b>
<b>SSN</b>	<b>Space Surveillance Network</b>
<b>RAAN</b>	<b>Right Ascension of Ascending Node</b>
<b>SODS</b>	<b>Semi-analytic Orbit Dynamics System</b>
<b>CLAPS</b>	<b>Close Approach Prediction Software</b>
<b>ISD</b>	<b>Inter- Satellite Distance</b>
<b>TCA</b>	<b>Time of Closest Approach</b>
<b>CMP</b>	<b>Covariance Matrix Propagation Method</b>
<b>NORAD</b>	<b>NORth American Aerospace Defense Command</b>



# Chapter 1

## Introduction

Human space activities for the past 60 years have created an expanding population of unwanted objects called space debris in the close vicinity of earth. The population of these space debris is still increasing at an alarming rate due to increased space activities and anti-satellite tests. Space junk or space debris consists of decommissioned and defunct satellites, pieces of space hardware, spent launch vehicle stages, and pieces or objects resulting from anti-satellite(ASAT) missions. These objects move around the earth in different geocentric orbits, posing a significant threat to the new missions planned and the existing active satellites. The danger is due to the high risk of collision between the space objects. Currently, the total number of space objects is around 41000, of which only 5100 are active payloads. If a collision happens between an operational satellite and an object with a cross-section larger than 10cm, the satellite can get destroyed resulting in a considerable loss.

In January 2007, China displayed its anti-satellite(ASAT) capability by creating a hyper-velocity collision of a KT-2 missile with an old weather satellite. Such demonstrations create large clouds of space debris which remain in orbit and pose a significant threat to active missions. The concept of space situational awareness was brought to the forefront after an unexpected accidental collision between an active

Iridium communication satellite and a non-functional Russian satellite debris.[1] The collision of a functioning satellite causes a lot of damage because it creates a new cloud of space debris and results in the loss of money and human efforts. Hence, to avoid such disastrous situations, the orbital state, i.e. position and velocity of every space object, must be accurately represented. Space situational awareness involves accurately representing space objects and mitigating unwanted hazards.

There are three regions in space where space debris is found: LEO Region (Lower Earth Orbit), MEO Region (Medium Earth Orbit), and GEO Region (Geosynchronous Earth Orbit). The LEO is below 2000km, the MEO is between 2000 km and 36000 km, and the GEO is at about 36000 km. Among these, most of the debris population is present in the LEO region. In the earth's orbit, certain regions in space have unique utility for satellite positioning. Thus such regions are becoming even more congested. The increased population of objects increases the chances of collision. Hence, steps need to be taken to track them properly. The planning of space missions needs to be done by considering this situation. Also, for existing active satellites, the proper awareness of the orbital state of space debris is useful as it can be used to conduct Collision Avoidance Manoeuvres(CAMs) to mitigate hazardous collisions.

## 1.1 Goals and Objectives

This work aims to get an estimate of the covariance matrix of relative positions of resident space objects in the most efficient manner. The relative positions of objects matter a lot to us because the number of space objects is increasing exponentially. This cluttering of the space around us is a threat to all future developments happening in space applications. Most resident space objects(RSOs) have a certain

amount of uncertainty associated with their position and velocity. But it is essential to know their exact locations to avoid fatal collisions. Here, the uncertainty related to the object is modelled as a Gaussian distribution and the covariance of relative positions is estimated. Other results associated with the position of objects are also determined. The miss distance is the distance between two objects at the time of the closest approach. The epoch at which two objects come the closest is called the time of closest approach(TCA). It is imperative to know this information to prevent any fatal collision that might happen due to the closeness of the objects. Since the number of objects in space is very high and rising with time, the covariance estimation needs to be done in the most computationally efficient manner. The conventional Monte Carlo(MC) method, the Extrapolated Single Propagation(ESPT) Method and the Covariance Matrix Propagation(CMP) method are implemented to compute the covariance matrix of relative positions. A comparative analysis is then carried out based on their computation time and the results it can generate. The orbit's perturbations are also considered to maximise the estimation accuracy while conducting the analysis.

## 1.2 Motivation

Due to this ever-increasing space activities, space debris is a huge problem for space research and space applications in future. In reality, there is a great threat for all active missions orbiting in the lower earth orbit as this area is the most crowded with space objects. To avoid a possible collision, it is most important to know the probability of such a conjunction event happening. The best way to estimate the collision probability of two objects is by determining the covariance of their relative positions. Hence, if we can find a way to model the uncertainty associated with the

objects' position and velocity in a proper way, this model can be used to estimate the relative position covariance matrix. Also, it is necessary to have an idea about how close two objects come in space and the time at which this happens. This can be achieved by propagating the orbit to future times and determining their positions in future.

## 1.3 Dissertation Layout

The rest of the thesis comprises the following chapters

**Chapter 2:** Literature review regarding the topic is discussed in detail.

**Chapter 3:** Methodology used to implement the idea is discussed in detail.

**Chapter 4:** All the results and simulations generated is shown and the conclusions made from the results are discussed in detail.

**Chapter 5:** The summary of the work completed and how this work can be expanded in the future is discussed here.

# Chapter 2

## Literature Review

### 2.1 Space situational awareness

Every space object orbiting around the earth has its own orbit defined. Space situational awareness involves accurate representation of these space objects at every point in time in order to avoid unwanted collision incidents[1]. It is very important to understand the orbit dynamics for this. To define a satellite orbit six parameters are required known as orbital elements or keplerian elements. These parameters define the elliptical orbit around the earth with the earth located at one focus. The keplerian elements are Orbit inclination, Right Ascension of Ascending node(RAAN), argument of perigee, eccentricity, semi-major axis, and mean anomaly.

The orbit ellipse lies in a plane called the orbital plane. The orbital plane goes through the center of the earth and is tilted at an angle with respect to the equatorial plane. This angle between the equatorial plane and the orbital plane is called the inclination. Inclination lies between 0 and 180 degrees. The RAAN is an angle measured at the center of the earth, from a reference point in space where the right

ascension is defined to be zero to the ascending node. It is in the range of 0 to 360 degrees. The argument of perigee is the angle between the line of apsides and the line of nodes. It lies between 0 and 360 degrees. Eccentricity tells the shape of the elliptical orbit. It has a range of 0 to 1. The semi-major axis is one-half the length of the larger axis of the elliptical orbit. Mean anomaly is an angle that changes from 0 to 360 degrees during one revolution. It is defined as 0 degrees at the perigee and 180 degrees at the apogee. These parameters are useful in finding the Cartesian coordinates of a satellite at a particular time. This information can be obtained by processing the TLE data [2].

TLE (Two-line element set) data consists of a list of orbital elements of a space object encoded together at a given time called the epoch. The data is in the form of two lines [3]. The first line contains identification and orbit information of the space object including the catalog number, epoch value, drag term, international designator. The second line contains orbit parameters. For lower earth orbit(LEO), the TLE has an error range of 1-2km and it is updated thrice in a day. For geostationary satellites, the error range is 10-30 km and it is updated once a day. So positioning errors always occur in between updates. The TLE inaccuracies need to be taken into account while using them for orbit estimation [4].

## 2.2 Tracking of space objects

The SST (Space Surveillance and Tracking ) is responsible for tracking space debris using radar and optical systems. SST systems discover new objects and catalog them for statistical purposes. Tracking involves follow-up and observation of orbit propagation of the cataloged objects. For space debris in low earth orbit(LEO), radar measurements have been used and for high earth orbit (HEO) optical measurements

are used. Ground-based radars have all-weather and day-night performances making them well suited to observe space objects. Various kinds of radars are used to track space debris in various modes. In tracking mode, the radar follows an object to gain data on angular direction, range, range rate, etc. From this data, orbital elements can be derived [5]. In beam parking mode the statistical information on the number and size of objects is found. Overall using radar measurements, the Altitude, describing the motion of an object, size, shape, orbital lifetime, ballistic coefficient, object mass, material properties can be found. In optical measurements, debris is detected by the telescope. This is done when the debris object is sunlit in the dark background of the sky. For LEO, this period is very limited and hence optical measurements are not effective. But for objects in HEO, the observations can be made at all times [6].

Based on the observations made, a complete preliminary orbit of a space object can be made. One main problem associated with the observations is to identify whether a set of data belong to the same space object or not. This is the correlation problem. After that, the orbit determination is done.[7] The observation batches that can be immediately assigned to a single object are attributable. It is represented as a 4-dimensional vector. A radar attributable vector is defined containing information from a radar observation at time  $t$ . From this attributable, the orbital elements are computed. The geometric structure of the orbits is sampled to generate virtual orbits in this method. The generated virtual orbits are then propagated in time to find other observations for the same object. The algorithm is named as virtual debris algorithm.

The observations made using radar and optical instruments are cataloged in the form of TLE (Two-line element set) data. TLE consists of a list of orbital elements of a space object encoded together at a given time called the epoch. As the name

suggests, the data is in the form of two lines. The first line contains identification and orbit information of the space object including the catalog number, epoch value, drag term, and international designator. The second line contains orbit parameters. For low orbit satellites, the TLE data have an error range of 1-2 km, and it is updated thrice in a day.[8] For geostationary satellites, the error range is 10-30 km and is updated once a day. As a result, positioning errors always occur in between the updates. Since TLE data is easily accessible and readily available, it is widely used as an input format for predicting future orbital tracks of space objects. All the information is cataloged for further use [7].

A space object catalog is maintained, which consists of orbital states of various space objects. The catalog is updated by sensor observations from SSN ( Space Surveillance Network). From these observations, the creation mechanism of space debris can be understood. This is essential for the safe operation and long-term sustainability of satellites. The purpose of the catalog is to provide values of current orbital elements. The number of cataloged objects is expected to grow exponentially in the coming years. The basis of orbital evolution and conjunction assessment is this catalog of objects. Various methods are also developed for catalog maintenance of space debris[9].

## 2.3 Orbit Propagation

Orbit propagation estimates the future state of motion of an object, whose orbit has been determined using past observations of orbital elements. Cowell's formulation is a method used to propagate the orbit to the future. In this formulation, the second-order differential equation is written for the position coordinates of the satellite.

The satellite motion is governed by

$$\ddot{\vec{r}} = \frac{-\mu}{|\vec{r}|^3} \vec{r} + a_p \quad (2.1)$$

where  $\vec{r}$  is the position vector of the satellite and  $a_p$  is the total perturbing acceleration. This orbit propagation method can be used to propagate orbit objects to the future and determine possibilities of collision in the future[10].

A multiscaling-based semi-analytic orbit propagation method was developed. Compared to the numerical method used earlier, this method improved the computational efficiency by 95 percent. In this method, the osculating elements are decomposed into mean elements and short periodic variations. First-order differential equations for mean element rate are produced by applying an averaging operator to the variation of parameter (VOP) equations. Short periodic variations are equated to the remaining part. The disturbing function is then separated into a mean component and short-periodic component depending on the time scale. A long-term scale for the mean component and a short time scale for the short-periodic component. This is the method of orbit determination used. From the equations formed, the first and second-order solutions are found by using the keplerian elements in the VOP equations of motion. This method can also be modified and used to find conjunction analysis [10].

### 2.3.1 Perturbations in Orbit

Another important factor to consider while propagating an orbit is the orbital perturbations. A perturbation is the deviation of an orbit from its regular path caused due to influence of external factors. Orbital Perturbations can be broadly classified into three types, third body perturbations, perturbations due to satellite operations,

and perturbations due to natural phenomena. A third body always influences the path of the object because of its gravitational effect. Satellite operations include changes in velocity or other manoeuvres initiated for some applications etc. This can bring about a drastic change in the future orbit of the space object. Natural phenomena include atmospheric drag, the effect of the earth's gravitational pull, solar radiation, etc. Atmospheric drag is the most important disturbance because it is an inevitable problem, and it affects each object differently. The effect of the drag will differ according to the size and shape of the object and also the position of the orbit. The closer the orbit is towards the earth's atmosphere, the more the effect of drag. The shape of the earth has a role in determining the gravitational force. Since the shape is not exactly spherical, the gravitational force exerted is not uniform resulting in changes in the values of orbital parameters RAAN and Argument of perigee[2].

## 2.4 Conjunction Events

When two objects in Earth's orbit come very close to each other or possibly collide with one another, such an event is called a Conjunction event. Conjunction assessment is the process of predicting a conjunction event by screening the ephemeris of the asset satellite against the space object catalog. The ephemeris is data showing calculated positions of a celestial object at regular intervals. Conjunction assessment is done in order to identify the risk of collision and to take necessary measures to avoid it. It is a crucial concern to the nations planning space missions. At the time of mission planning and selection of orbital bands, the results of conjunction assessments need to be taken into consideration. The risk associated with a specific orbit can be found out by using statistical conjunction assessment [3].

There are various methods of estimating the number of possible conjunctions for a body. In one method, the gross orbital properties of space objects were taken as a sample space, and from this, risk analysis was done. Mostly conjunction estimates are carried out in terms of close proximities. Here, a primary object is considered (which will be an operational satellite), and other large-sized cataloged objects are taken as secondary objects. The TLE information for all secondary objects is collected. Using this information, the trajectories of secondary objects are propagated for a few days. Space objects that come within a critical distance from the primary object are identified. This critical distance is determined by warning boxes which are approximately 25 km along the track of orbit, 5 km radially from Earth, and 5 km across the track of orbit. The objects which come inside the warning box are assessed again to determine if any of them come inside a maneuver box. In such a situation, the primary object needs to initiate a maneuver to avoid a collision [3]

A step-by-step procedure to carry out statistical conjunction analysis is also there. The aim here is to find the number of objects passing through an altitude bin between A km and B km in a year. Initially cataloged objects which are not at all present in the bin are filtered out by apogee and perigee filtering. Objects with perigee greater than B km and objects with apogee less than A km are filtered out. Other objects pass through this altitude bin at least 2 times on average. From this, the number of objects in a cubic volume in a year is found. Any warning box conjunctions happening are obtained by considering the box volume and altitude. In this way number of conjunctions in a year is estimated.

The drawback of the above method is the TLE data inaccuracy. Also, the spacecraft orbit always has some dispersion on the orbital parameters. To account for these uncertainties, the Monte Carlo approach can be used to find the expected number of conjunctions. It is a simulation technique that assesses the performance deviations

when input conditions are varied. The inaccuracies in TLE are selected randomly based on normal distributions within the 3 sigma values. For all parameters, Gaussian distribution is assumed. The TLE epoch is propagated to a common epoch and all the parameters are converted into position and velocity components. Random perturbations are added to the parameters as per dispersion levels. Now the parameters are converted back to Apogee, Perigee, and Inclination. On this, the statistical conjunction algorithm is applied to obtain the number of conjunctions happening in an altitude bin. From the observations made it can be inferred that the inaccuracies in TLE did not affect the result. Thus, the Monte Carlo approach is very precise and easily implementable. But a drawback of this method is slow computing speed when propagating one epoch to another.

The challenge is to do the conjunction analysis for hundreds of thousands of space objects in an efficient manner with good accuracy. In a perturbing environment, the orbital error shows the accuracy of the object's state. This can be utilized for orbit propagation for conjunction analysis. This overcomes the low computing speed of the Monte Carlo approach because here the orbital error is propagated in a way that agrees with the non-linear orbit dynamics system (ODS). The probability density function (PDF) and statistical state moments such as mean, covariance, skewness, and kurtosis depict the uncertainty of a state  $x$  at epoch  $t$ . Using error propagation, the exact statistical description of state  $x$  at a future time can be obtained. This is done by propagating the orbital error using non-linear propagation methods such as the Fokker-Plank equation, Gaussian mixture model, etc. But again these non-linear propagation methods have their own drawbacks leading to low computational efficiency. There also exist linear propagation models. Here the non-linear dynamics problem is simplified by assuming initial errors as Gaussian. Even though the linear techniques are efficient, the results do not agree with those predicted by non-linear

propagation models.

To overcome the computational problem, the semi-analytic satellite theory (SST) was explored. Here the perturbing forces acting on the object are studied and the osculating orbital elements are separated into two components, the mean elements, and the short periodic elements. This reduces the non-linearity of the mean elements[11]. The orbit is thus propagated in a semi-analytic orbit dynamics system (SODS). The mean equations govern the slowly varying trend of orbit elements thus removing the non-linearity of orbit dynamics. The mean quotations are numerically integrated with a large step size to propagate all small errors in the initial orbit. The short periodic terms are solved analytically. This method of solving SODS is called the multiscaling technique. The performance of the SODS method is compared with the Monte Carlo approach to compare the computational efficiency achieved. The results showed a 95 percent improvement in computational efficiency [10].

### **2.4.1 CLAPS Tool for conjunction analysis**

Close Approach Prediction Software (CLAPS) is a new tool used for conjunction analysis of operational satellites of ISRO. This software can carry out conjunction analysis for all the operational satellites with other cataloged space objects. The aim is again to increase the computational efficiency. Here, some pre-filters are used and many object pairs are screened out. The algorithm to compute the collision probability is applied to only those object pairs which are passed by all filters. For close approach analysis, the inter-satellite distance (ISD) between the operational satellite and other cataloged objects is computed. The orbit for each pair is propagated for a specified duration, and ISD is found out. If the ISD goes below a specific threshold value, then these object pairs are considered for the calculation of collision

probability. The pre-filters are used to rule out irrelevant object pairs from the calculation of computational efficiency. The first filter used here is the Perigee/Apogee filter. For many object pairs, the relative geometry of their orbits never crosses each other. The Perigee/Apogee filter finds out such pairs are eliminated. The next filter used is the Smart-sieve filter. The concept used to design this filter is the fact that the relative velocity between two orbiting objects cannot exceed two times the escape velocity. Based on this, a threshold distance is identified. A critical area around the primary object is also identified. If the initial distance to the critical area is higher than the threshold distance, then the object cannot enter and exit the critical volume within a specified time frame. So if objects are separated by more than this threshold distance, then they are filtered out. The sieves have very high efficiency and are very useful for eliminating a large number of objects [12].

Since the aim is to reduce the computational load, the ISD is calculated only in the end after the application of all filters. The relative distance function method is used to determine the close approach as it is a much-improved method compared to conventional methods. Position vectors for the primary and secondary objects are considered at a particular time  $t$ . The relative distance vector is found from the position vectors and its time derivative is found out. The distance function is found by taking the dot product of the relative distance vector with itself. Their time derivatives are found. The second time derivative is equated to zero to find the local minimum which is the closest approach distance. Only those objects which pass through the filters are subjected to conjunction detection by the relative distance function. If the object pairs are found to be in close proximity, ie if they are a threat pair, then the analysis is repeated and the collision probability of the same is calculated[13].

For conjunction risk assessment, the two most important criteria to be considered

are closest approach distance and collision probability. To determine collision probability, the estimated state vector and initial error covariance matrix of the primary object and secondary object at their epoch are needed. The determined state vector and error covariance of each object are propagated using orbit and covariance propagation models. The time of the closest approach and corresponding state vectors of the object pairs are obtained using an appropriate close approach analysis method. With this, a safe radius of two objects is calculated. From this information, the collision probability is calculated for the two objects[14].

Calculation of collision probability is done for only those object pairs which pass through all filters and whose relative distance function proves it to be a threat pair. This is to reduce the computational load. Here, it is assumed that the relative position of object pairs with respect to each other is Gaussian distributed. The covariance matrix corresponding to this is found out and then the three-dimensional PDF (Probability density function) is found. It is then volume integrated to find out the collision probability. The dynamic 3D problem is reduced to a static 2D problem. For this calculations are done in the 2D conjunction plane. The conjunction plane is the plane perpendicular to the relative velocity vector at the time of conjunction. A two-dimensional expression for probability is found and it is solved to obtain the collision probability. From the results, it is clear that the software predicts all close approaches with high efficiency and accuracy[15].

## 2.5 Collision Probability

The collision probability is calculated in order to plan and take proper risk mitigation measures. Hence, collision avoidance procedures are an integral part of satellite operations. Such collision avoidance measures can be aided by applying suitable

machine learning (ML) models. This will help in predicting the collision risk over time. The European space agency (ESA) released a unique dataset that contained information about close approach events. The data set was in the form of conjunction data messages (CDMs) collected from 2015 to 2019. A machine learning challenge was hosted inviting participants to predict the final risk of collision at the time of closest approach. The datasets, results, and various other factors were analyzed to highlight the problems in collision avoidance systems and to find the best use of ML methods in collision avoidance systems[16].

The dataset used contained information in the form of CDMs in ASCII format. Here the monitored space object is termed as the target satellite and the secondary object as chaser satellite. In the CDMs, various attributes of a close approach like time of close approach, the identity of the objects, their velocity and position and, their associated covariances. In the data processing part, the CDMs are processed and the risk estimates are found. After collecting CDMs regularly, various uncertainties get smaller and there is more refined knowledge about the close approach. A threshold value is assigned for the collision risk, if the value exceeds the threshold then a collision avoidance maneuver needs to be initiated some days prior to the close approach. Even though a risk value associated with each CDM is available, it is not propagated to find the risk value into the future[17].

The aim is to find the associated collision risk and to decide whether a collision avoidance maneuver needs to be performed or not. With the available CDMs, the future collision risk needs to be predicted. The competition was designed to forecast the collision risk from the conjunction events database. For the competition purpose, the data was processed in a particular manner. Some events where the spacecraft actually performed a collision-avoidance maneuver were not considered because from these CDM data, the collision risk cannot be found. The data was

---

also made anonymous by transforming absolute timestamps, position, and velocity values into relative values. The mission names were also removed and a random identifier was assigned. The database was then divided into training and test sets in such a way that events that correspond to useful scenarios appeared in the test set. The competition had two main objectives for the participants. The first one is to correctly classify the events into high and low-risk events, the second is to predict the risk value of the events. Since the matter of interest here is collision avoidance, the false negatives are much disastrous than false positives. As a result, their occurrences need to be penalized more. Also, in the dataset, the number of high-risk events is much lesser than the number of low-risk events making this a highly unbalanced problem.

Based on the problem, the methods adopted by each of the teams in the competition were studied and analyzed. Also, the various problems faced by the teams due to the unbalanced nature of the dataset were studied. From the results, it was inferred that naive forecasting models have good performances and can be established as a benchmark. However, ML models can improve upon this benchmark and can be used to improve the decision-making process in collision avoidance systems [18].



# Chapter 3

## Methodology

Initially, TLE information for a list of space objects for a particular date range was downloaded from the website [www.spacetrack.org](http://www.spacetrack.org). The TLE information for each space object contained information about the values of its orbital elements, the drag coefficient, etc of the satellite. The 6 orbital elements include eccentricity, semi-major axis, RAAN, Argument of Perigee, Inclination associated with the listed space object at the latest time of TLE availability, and mean anomaly. Utilizing the information from the TLE data, 3D orbit visualization of the list of space objects was made. Visualization of orbits is a preliminary step toward finding the collision probability.

TLE data is processed first and orbital elements are extracted from it by processing it. The orbital elements are stored in a CSV file for easier handling of the data and are used to form the orbit object. Orbit object is useful in the visualization of orbits and also for orbit propagation. It is also used to determine the position of the object at a particular epoch value.

### 3.1 Initial Implementation steps

A primary object is selected and all other objects in space are considered secondary objects. The TLE information for the primary object is downloaded and processed. The orbital elements information obtained from the TLE data is then stored in a CSV file. Similarly, for all the secondary objects present, the same procedure is followed. In this way, the list of secondary objects and their orbital information is formed. Using this list of objects and their orbital information, each object was represented in the form of an orbit object.

The orbit object representation makes it easier to visualize and understand the dynamics of every orbiting object. Hence the primary object and all the secondary objects are represented in the form of orbit objects. Now, the relative position of the primary with respect to each of the secondary objects is calculated. This is then stored in the form of a list. The relative position data is then used to form the covariance matrix which in turn can be used to find the collision probability between the primary object and each secondary object.

### 3.2 Filtering of irrelevant objects

Since there are around 18,000 objects in space, and the process of determining the covariance is computationally heavy, calculating the value of covariance matrices is quite time-consuming. In these circumstances, it is important to find out ways to reduce the computational complexity.

### 3.2.1 Date based Filter

On inspecting the epoch values of primary objects, it is observed that they exist in the space for a specific range of dates. While calculating the covariance, it was observed that for objects which didn't exist in the same time period the values are coming in as negligible. There is no point in considering such secondary objects in the computation. Considering this, while calculating the covariance matrix, only those secondary objects which are present during the same period are taken. Objects present at other dates are filtered out during the data processing itself.

### 3.2.2 Apogee-perigee Filter

Apogee-perigee filtering is also used for filtering the secondary objects. Using the values of the semi-major axis and the eccentricity for an orbit, the apogee and perigee height can be calculated. Two objects will only collide if their orbit paths cross with each other. This will only happen if the apogee height of one object is lesser than the other and its perigee height is greater than the other or vice versa. Utilizing this criterion, a large number of objects are filtered out, reducing the computational complexity to a great extent. The advantage of the apogee perigee filtration is that after applying the filter, it took only 9.7 seconds for finding the covariance matrix values for a set of 150 objects whereas it was taking about 3 minutes for the same before applying the filter.

## 3.3 Orbit Propagation

Orbit propagation is the prediction of orbital characteristics of a satellite to a future date using the current available orbital data. The orbit object formed is propagated

to the future using a propagator called Cowell propagator. The relative position values of the primary and secondary are used to propagate their corresponding orbit object to the future. A set of times is used as an array and the propagation is done to these set of times. Using this propagated orbit object, the positions and velocity of the primary and secondary at a set of future times are obtained in the form of cartesian values  $(x,y,z,vx,vy,vz)$ . This is then used to calculate the Euclidean distance between the primary and the secondary object for the array of times. The set of Euclidean distances is used to find the minimum miss distance, ie the closest the two objects come. At this point, the covariance matrix is evaluated. The miss distance, the epoch value, and covariance are found at the time of the closest approach and stored in the form of a CSV file. This is called the CDM (Conjunction data message). The CDM contains information about the closest approach of two objects. It includes the time of closest approach, the miss distance, and the covariance associated with the relative position of primary and secondary object at that time.

The inter-satellite distance in kilometers is plotted with respect to the time to visualize the change in position of the primary with respect to the secondary. This is very crucial in determining how close two objects come in the future and to determine the likelihood of a collision.

### 3.3.1 Adding Perturbations while propagating

Another important point to be considered while propagating the orbit to the future is orbital perturbations. A deviation of a system or a moving object from its regular path caused by outside influence is called a perturbation. Perturbations can happen due to a third body, or due to change in orientation of the orbit due to satellite operations, or by natural phenomena such as solar radiation, atmospheric drag,

the gravitational effect of the earth. The atmospheric drag affects each satellite in a different way and is defined by the atmospheric drag coefficient  $B^*$  which is available in the TLE data of the satellite.

The shape of the earth is an oblate spheroid and it also affects the orbit of the satellite. There are perturbing forces called J2 and J3 Perturbations. The term J2 and J3 are from an infinite series math equation that describes the effect of the earth's shape on the gravity of a planet. J2 and J3 coefficients have the strongest effect on the orbits. The J2 perturbations affect the RAAN and Argument of perigee. If earth were to be modeled as a perfect sphere, then the gravitational field would have been uniform and the RAAN and Argument of perigee wouldn't change. Since the earth is not a perfect sphere, these perturbations must be accounted for.

After taking into account all the perturbations ie J2, J3, and Atmospheric drag, the propagation of the primary and the secondary object is carried out, and using these propagated values of the orbit object the CDM is formed. Since the effect of perturbations is also taken into consideration, the information present in the CDM, ie the miss distance and time of the closest approach is now much more accurate.

### 3.4 Estimating with better accuracy

It is important to estimate the covariance values with better accuracy because a miscalculation can cause fatal damage to important space assets. The orbit object created using the orbital element values obtained from TLE data is not completely accurate because TLE data has inaccuracies. To mitigate this problem, two steps are taken, the first one is sampling the orbital element values to a large number of data points and the second one is estimating the accurate TLE from all the available set of TLEs.

### 3.4.1 Orbit Sampling

The various possibilities of orbit object positions are formed by sampling the orbital element values to a large number of data points. This is done for both the primary object and all the secondary objects. In this way, a large number of sample points are formed for both primary and secondary objects. The position difference between two possible orbit objects is calculated and made into a list. Using these values, the covariance matrix is generated. This covariance matrix will give a far better estimate of the collision probability value between the objects.

### 3.4.2 Estimating the accurate TLE

Initially, while carrying out the orbit propagation, the TLE obtained from [www.spacetrack.org](http://www.spacetrack.org) for any object was considered as it is and the orbit object created from it was propagated to the future. But on visualising the samples of orbit objects, it was observed that the samples were spread out and the standard deviation was high. Hence it was imperative that the data used to create the samples had inherent inaccuracies and that was the reason for the anomaly in the visualisation of samples. It is very important to solve this problem because the TLE data is the base of the work and every computation is done by using the TLE data. In effect, the errors in TLE get propagated and reflect in the covariance values.

To solve this problem, the following steps are taken. For each TLE data downloaded, the epoch associated with it is determined. The orbit object is determined at that point using the TLE. Now all these orbit objects are propagated to a single epoch at present. From these orbit objects, the accurate orbital elements are determined and they are used to create the samples. To verify that the TLE inaccuracy issue

has been resolved, the samples are visualised and their spread is determined using their standard deviation values.

### 3.5 Covariance Matrix Estimation

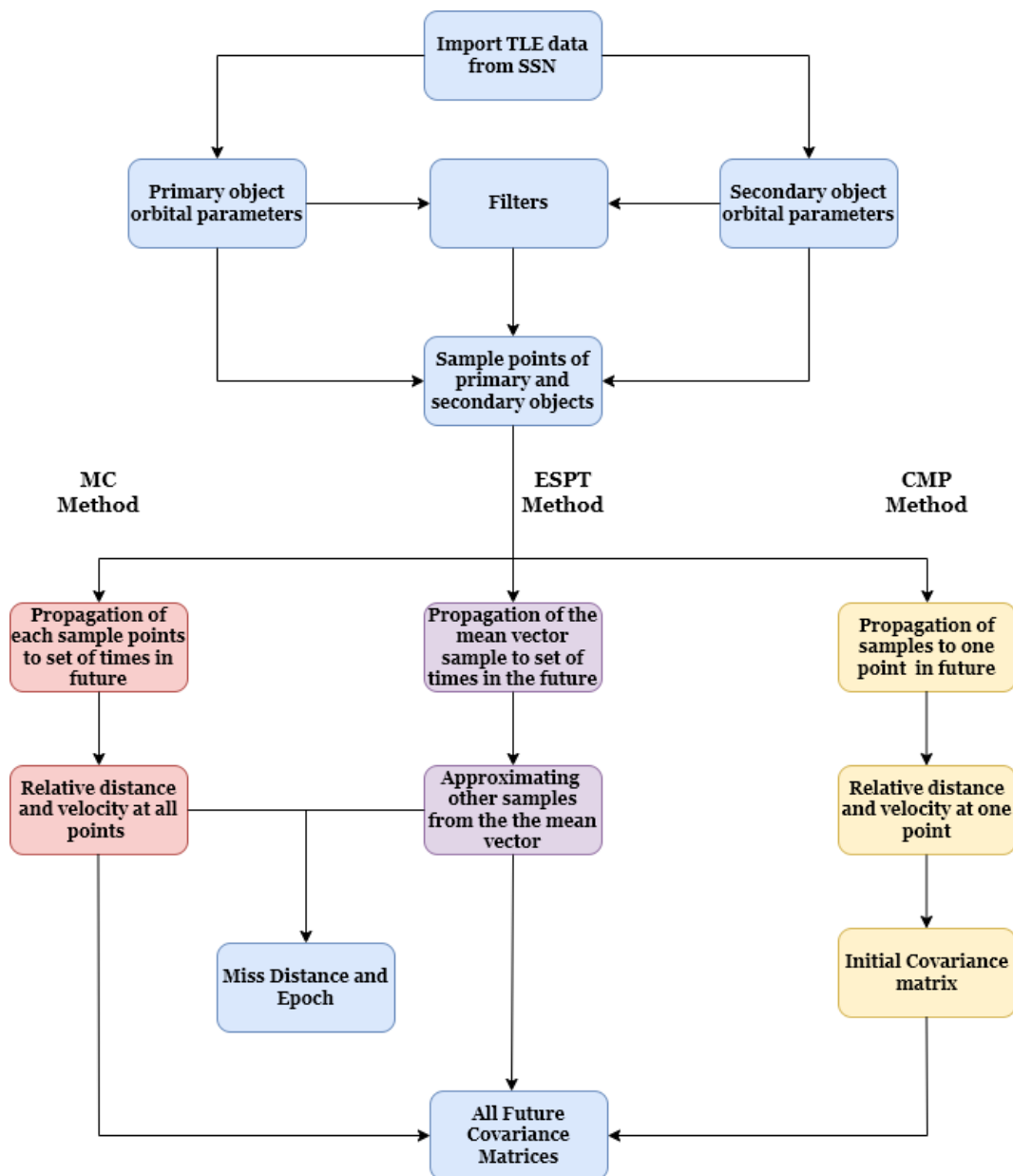


FIGURE 3.1: Block diagram depicting flow of implementation

The aim is to estimate the covariance associated with the relative positions of the primary with respect to the secondary at a set of times in the future. This information is crucial, as it gives an insight into the possibility of a conjunction event happening between two space objects. Also, it is essential that this covariance is estimated in the best possible way. Three methods are identified and compared based on the computation time taken to estimate the covariance matrix and its utility, i.e. the kinds of information it can generate. The three methods have been implemented, and their methodology is explained in detail. Figure 3.1 shows a general block diagram which depicts the flow in which the implementation is done.

### 3.5.1 Monte Carlo Method

This method, also known as multiple probability simulation, is primarily used to estimate probable outcomes of an event with associated uncertainties. Initially, a model is built by assuming a probability distribution for the event or variable that has an uncertainty associated with it. Usually, the uncertainty is assumed to have a normal distribution. After building the model, the result is repeatedly calculated using a different set of random samples. Typically, this is repeated a large number of times to get the maximum possible likely outcomes.

In this work, the Monte Carlo Method is implemented to estimate the covariance associated with the relative positions of the primary object with respect to the secondary object. For the primary object, the orbital parameters are obtained using a large set of TLE values, which are sampled to a large number of data points for applying the Monte Carlo approach. Similarly, the same procedure is followed for the secondary object. Samples of orbit objects are created using the data points generated. These samples are visualised to verify our hypothesis that they will

follow the normal distribution. Now the samples are propagated to a set of times in the future, considering the perturbations. The relative position and velocity values of the primary with respect to the secondary are calculated, which in turn is used to calculate the covariance matrix.

### 3.5.2 Extrapolated Single Propagation Method

In this method, multi-dimensional Richardson extrapolation is used to approximate the samples of state vectors at future time instances. Only the mean state vector is propagated and other samples are approximated from the mean term using Taylor series expansion[19].

Consider the state vector  $X$  at time  $t$ ,

$$X_i(t) = X^{\hat{}}(t) + \Delta X_i, (i = 1, 2, 3, \dots, n) \quad (3.1)$$

$i^{\text{th}}$  sample state vector at time  $t + \delta t$  will be,

$$\begin{aligned} X_i(t + \delta t) &= F(t, X_i(t)) \\ &= F(t, X^{\hat{}}(t)) + D_{\Delta X_i} F + \frac{D_{\Delta X_i}^3 F}{2!} + \frac{D_{\Delta X_i}^3 F}{3!} + \dots \end{aligned} \quad (3.2)$$

Now,

$$D_{\Delta X_i} F = \left. \frac{\partial F}{\partial X_i(t)} \right|_{X=X^{\hat{}}(t)} \quad (3.3)$$

$X_i(t + \delta t)$  can be approximated as,

$$\begin{aligned} X_i(t + \delta t) &\approx F(t, X^{\hat{}}(t)) + D_{\Delta X_i} F \\ &\approx X_0(t + \delta t) + \left. \frac{\partial F}{\partial X} \right|_{X=X^{\hat{}}(t)} \Delta X_i \end{aligned} \quad (3.4)$$

$\frac{\partial F}{\partial X}$  can be evaluated using Jacobian,

$$\frac{\partial F}{\partial X} = e^{J\delta t} \quad (3.5)$$

where  $J$  is the Jacobian of  $F$  evaluated at  $X = X\hat{(t)}$ .

Consider the state matrix represented as,

$$X = \begin{bmatrix} \vec{r} \\ \vec{v} \end{bmatrix} \quad (3.6)$$

$\vec{v}$  is the velocity vector of the orbit object as well as the differential of the position vector of the orbit object. Hence, we can write  $X$  as,

$$X = \begin{bmatrix} \vec{r} \\ \dot{\vec{r}} \end{bmatrix} \quad (3.7)$$

Differential of state matrix,  $\dot{X}$  can be represented as,

$$\dot{X} = \begin{bmatrix} \dot{\vec{r}} \\ \ddot{\vec{r}} \end{bmatrix} \quad (3.8)$$

This can be written as,

$$\dot{X} = G(X) \quad (3.9)$$

Then,

$$\frac{\partial G}{\partial X} = \begin{bmatrix} \frac{\partial \dot{\vec{r}}}{\partial \vec{r}} & \frac{\partial \dot{\vec{r}}}{\partial \vec{v}} \\ \frac{\partial \ddot{\vec{r}}}{\partial \vec{r}} & \frac{\partial \ddot{\vec{r}}}{\partial \vec{v}} \end{bmatrix} \quad (3.10)$$

This can be simplified as,

$$\frac{\partial G}{\partial X} = \begin{bmatrix} 0_{3 \times 3} & I_{3 \times 3} \\ -\frac{GM}{r^3} I_{3 \times 3} & 0_{3 \times 3} \end{bmatrix} \quad (3.11)$$

Finding the Jacobian is basically evaluating  $\frac{\partial G}{\partial X}$  matrix,

$$\frac{\partial F}{\partial X} = e^{\frac{\partial G}{\partial X} \delta t} \quad (3.12)$$

By applying this the mean state vector is propagated to a set of times in the future. After the propagation of the mean state vector, the other samples at each time step are calculated by first-order Taylor series approximation [19]. This approximation is possible only when the  $\delta t$  is taken as a very small value.

In this work, covariance associated with the relative position of the primary with respect to the secondary is estimated using the ESPT method. Samples of orbit objects of the primary and the secondary are created using the data points generated from the orbital parameters. The position and velocity vectors of the samples are evaluated and a mean state vector is generated from the samples. Only the mean state vector containing values of  $x, y, z, v_x, v_y,$  and  $v_z$  is propagated to a set of times in the future. Since all the samples are not propagated and only the mean state vector is propagated, it is expected to take lesser computation time than the conventional Monte Carlo Method. Once the mean state vector is propagated, the other samples at every time in the set of times are evaluated to obtain the state vectors of individual samples. This same process is repeated for both the primary and the secondary objects to obtain their respective state vectors. This data is then used to find the relative position and velocity vectors and the covariance matrix is calculated using this.

### 3.5.3 Covariance Matrix Propagation Method

In this method, the concept is to create an initial covariance matrix by using the Cowell propagator and then estimate the rest of the covariance matrices from the means of state matrices [20]. The state matrices of primary and secondary are propagated separately to the future and their difference is computed to obtain  $\Delta X$ .

The state matrix can be represented as,

$$X = \begin{bmatrix} \vec{r} \\ \vec{v} \end{bmatrix} \quad (3.13)$$

$\vec{v}$  is the velocity vector of the orbit object as well as the differential of the position vector of the orbit object. Hence, we can write  $X$  as,

$$X = \begin{bmatrix} \vec{r} \\ \dot{\vec{r}} \end{bmatrix} \quad (3.14)$$

Consider  $r_p$  and  $r_s$  as the position vector of the primary object and secondary object respectively. From this, the state matrix for the primary object can be written as,

$$X_p = \begin{bmatrix} \vec{r}_p \\ \dot{\vec{r}}_p \end{bmatrix} \quad (3.15)$$

Similarly, the state matrix for the secondary object can be written as,

$$X_s = \begin{bmatrix} \vec{r}_s \\ \dot{\vec{r}}_s \end{bmatrix} \quad (3.16)$$

To get the relative position difference between the primary and the secondary,  $\Delta X$  needs to be evaluated.  $\Delta X$  can be evaluated from the difference of state matrices

$X_s$  and  $X_p$ .

$$\Delta X = X_s - X_p \quad (3.17)$$

$$\Delta X = \begin{bmatrix} \vec{r}_s - \vec{r}_p \\ \vec{r}_s - \vec{r}_p \end{bmatrix} \quad (3.18)$$

Using the  $\Delta X$  matrix at time  $t$ , we can estimate the  $\Delta X$  at  $t + \delta t$  from equation 3.19

$$\Delta X(t + \delta t) = \Phi \Delta X(t) \quad (3.19)$$

where  $\Phi$  is the state transition matrix.

$$\Phi = e^{\frac{\partial \Delta \dot{X}}{\partial \Delta X} \Delta t} \quad (3.20)$$

To evaluate  $\Phi$  we need to evaluate  $\Delta \dot{X}$  and  $\frac{\partial \Delta \dot{X}}{\partial \Delta X}$

$$\Delta \dot{X} = \begin{bmatrix} \vec{r}_s - \vec{r}_p \\ \vec{r}_s - \vec{r}_p \end{bmatrix} \quad (3.21)$$

$$\Delta \dot{X} = \begin{bmatrix} \vec{r}_s - \vec{r}_p \\ -\frac{GM\vec{r}_s}{r_s^3} + \frac{GM\vec{r}_p}{r_p^3} \end{bmatrix} \quad (3.22)$$

$$\frac{\partial \Delta \dot{X}}{\partial \Delta X} = \begin{bmatrix} \frac{\partial \vec{\Delta r}}{\partial \Delta r} & \frac{\partial \vec{\Delta r}}{\partial \Delta r} \\ \frac{\partial \vec{\Delta r}}{\partial \Delta r} & \frac{\partial \vec{\Delta r}}{\partial \Delta r} \end{bmatrix} \quad (3.23)$$

Solving equation 3.23,

$$\frac{\partial \Delta \dot{X}}{\partial \Delta X} = \begin{bmatrix} 0_{3 \times 3} & I_{3 \times 3} \\ 0_{3 \times 3} & 0_{3 \times 3} \end{bmatrix} \quad (3.24)$$

From these values  $\Phi$  can be evaluated as,

$$\Phi = e^{\begin{bmatrix} 0_{3 \times 3} & \Delta t I_{3 \times 3} \\ 0_{3 \times 3} & 0_{3 \times 3} \end{bmatrix}} \quad (3.25)$$

The Future covariance matrices can be evaluated by using the initial covariance matrix and value of  $\Phi$  as shown in equation 3.26

$$P_{\Delta X}(t + \delta t) = \Phi P_{\Delta X}(t) \Phi' + Q \quad (3.26)$$

This concept is implemented in Python and the covariance matrix that is evaluated at the initial propagation point is passed to the future covariance function and the rest of the covariance matrices are evaluated there. Since this method does not involve the propagation of samples to every point in the future, this method is expected to take the least computation time.

# Chapter 4

## Results

### 4.1 3D orbit visualisation

The 3D orbits for various space objects are determined using the TLE values obtained from the [www.spacetrack.org](http://www.spacetrack.org) website. Initially, the orbital elements of each space object are determined from the TLE data. Then their mean and standard deviation is calculated. The orbit is determined and visualised using the computed values. Figure 4.1 shows one of the visualisations.

In the figure, the orbit followed by the object is depicted, and the position of the object at one point in time is shown. The 3D visualisation of orbits gives us a better understanding of the path traversed by an RSO in space. This is the first step toward modelling the uncertainty associated with the position of an RSO.

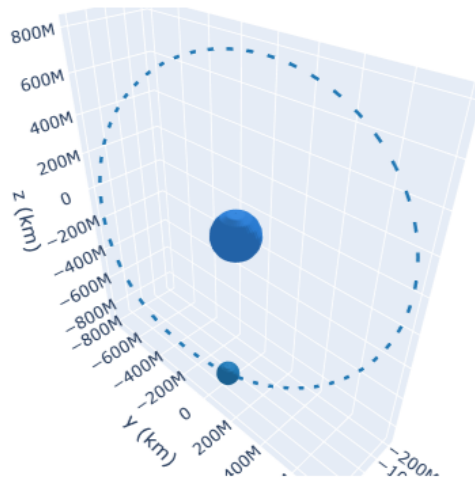


FIGURE 4.1: 3D orbit of the object with NORAD CAT ID 43939

## 4.2 Inter-satellite distance

Inter-satellite distance(ISD) refers to the euclidean distance between two RSOs in space. One RSO is considered the primary object, and all other objects in space are considered secondary objects. The inter-satellite distance between the primary object and one secondary object is determined at each point of time to which the orbits are propagated. The variation of inter-satellite distance with time is visualised by plotting it.

### 4.2.1 General Plots of ISD with time

Here, one space object with NORAD CAT ID 43212 is considered the primary object and all other objects left after filtration are considered secondary objects. The miss distance and epoch value at the time of closest approach(tcp) for secondary objects

with a high chance of collision is generated as a CSV file and stored. The plot of inter-satellite distance with time is generated. This plot tells us how an object pair moves about in space and the situations where it could result in a conjunction event. The plots are depicted in Figures 4.2 and 4.3.

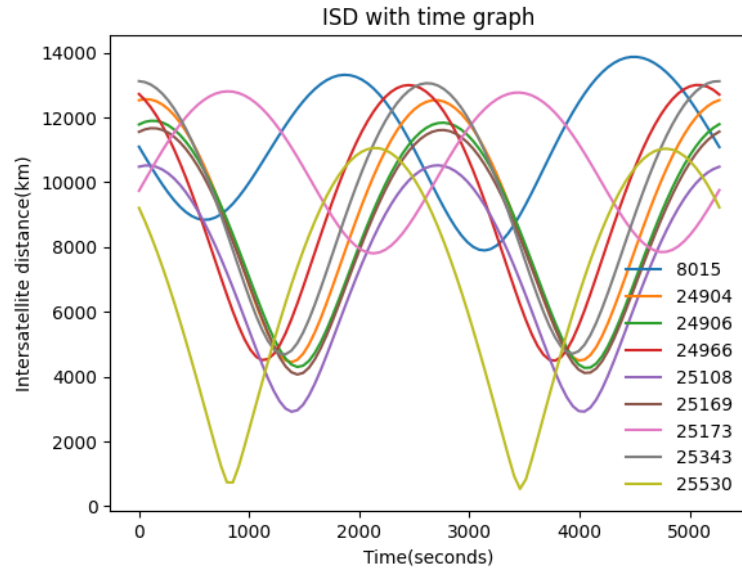


FIGURE 4.2: Inter-satellite distance with perturbations plot 1

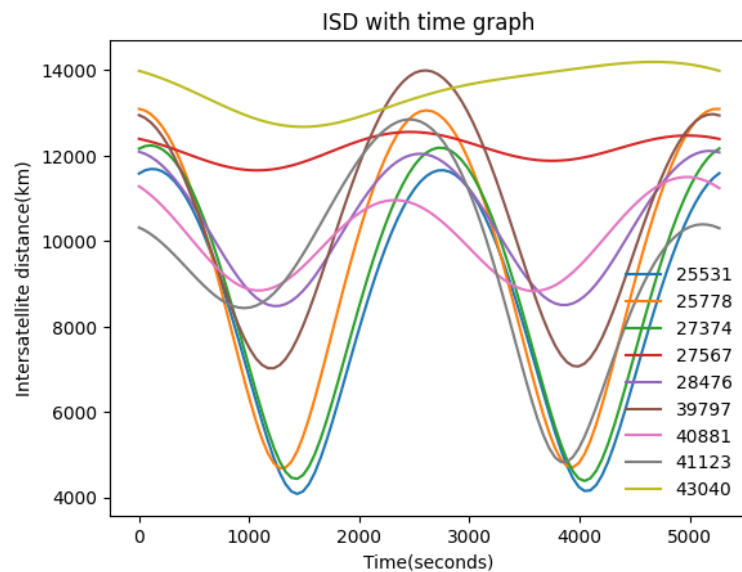


FIGURE 4.3: Inter-satellite distance with perturbations plot 2

The inter-satellite distance plot with respect to the time indicates that two objects come very close at the time of closest approach, then move apart and again come closer as the objects traverse through the space. This process keeps on repeating.

For any two objects in space, the collision probability will be highest, and the miss distance will be smallest during the time of the closest approach. A collision event is more likely at this point when the inter-satellite distance decrease. Therefore, the miss distance value has a significant role in predicting probable collision events. Even a tiny error in the miss distance is fatal. Hence it is imperative to bring accuracy in the calculation of miss distance.

#### 4.2.2 Box Plots of ISD with time

Considering one primary object and one secondary object, box plot of inter-satellite distance with respect to time is generated for both the ESPT Method and Monte Carlo Method. From the box plot, we can get a great insight into how the data is spread out.

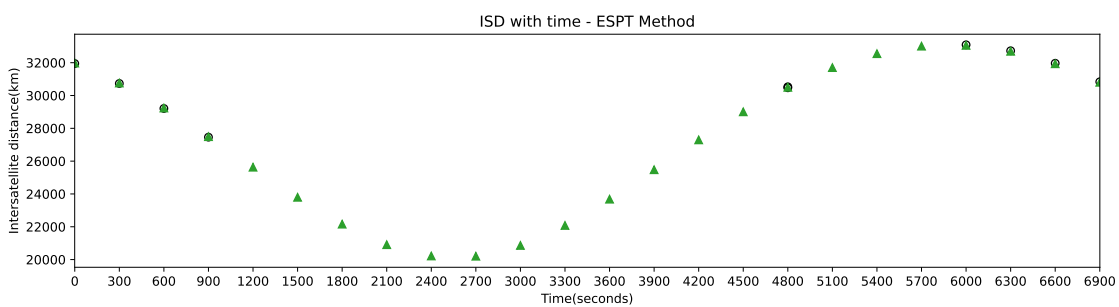


FIGURE 4.4: Box plot of inter-satellite distance in ESPT method

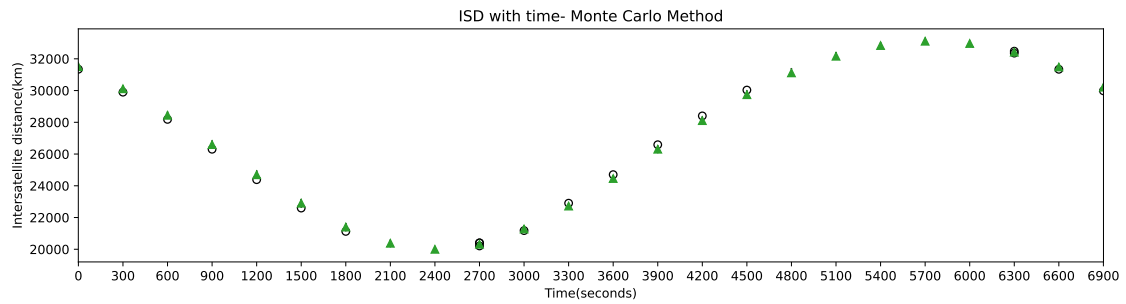


FIGURE 4.5: Box plot of inter-satellite distance in MC method

### 4.3 Orbit Propagation visualisation

Orbit Propagation is carried out for the object with NORAD CAT ID 46137. In the Monte Carlo Method, samples are created first, and they are propagated separately. In the ESPT method, only the mean is propagated, and the samples are recreated after propagation. The plot of the position of the samples with respect to the earth after every 300 seconds is generated. This plot gives us a better visualisation of how the samples are distributed as we propagate forward in each step. The plot is created using the data generated in CSV format after the propagation is carried out using each method.

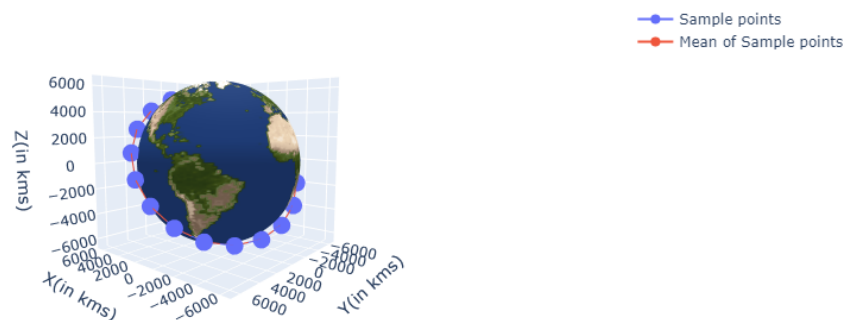


FIGURE 4.6: Samples Propagation - ESPT Method

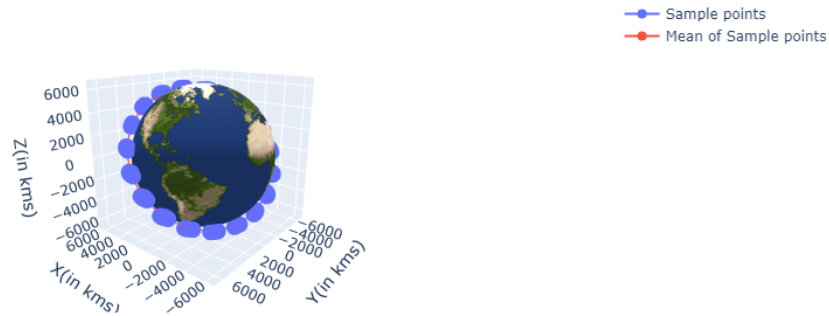


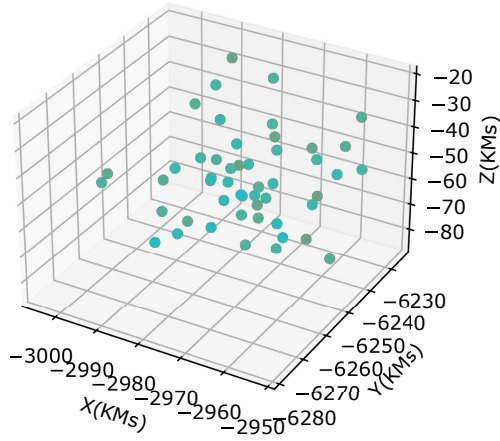
FIGURE 4.7: Samples Propagation - Monte Carlo Method

## 4.4 Samples Plot

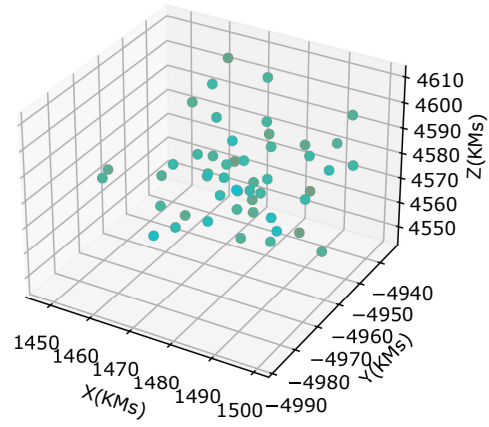
Sample points of the orbit object represent various probable locations of the orbit based on the available TLE data. When all the probable locations are considered while calculating the probability of collision, it increases the accuracy of the calculation.

### 4.4.1 ESPT Samples

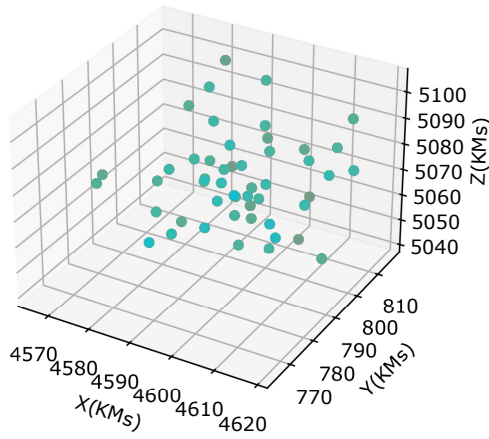
Sample points of orbit object are propagated to a set of times in the future using the ESPT Method. Here a mean state vector is formed and the state vector is propagated to every second until the propagation is completed for 7200s. Using this data, the samples are reconstructed at every point in time. The recreated samples position is determined after every 900s and a plot is generated.



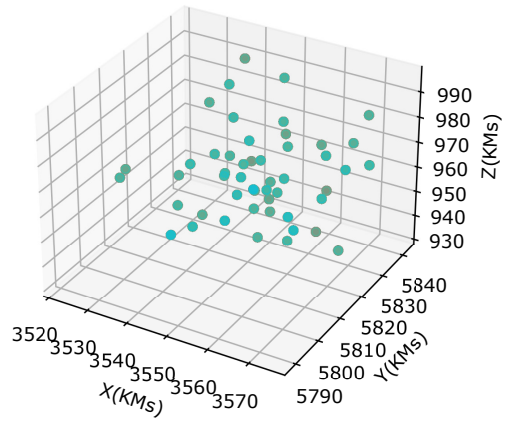
(a) ESPT samples at timestamp = 1s



(b) ESPT samples at timestamp = 901s

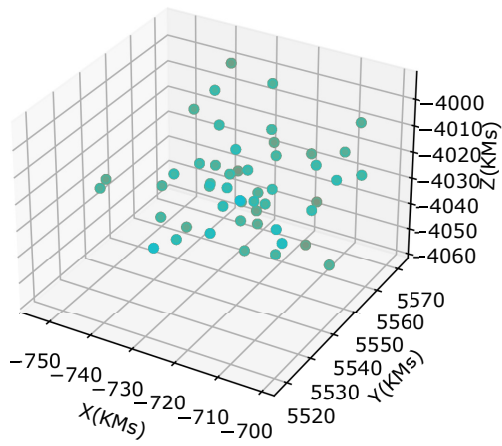


(c) ESPT samples at timestamp = 1801s

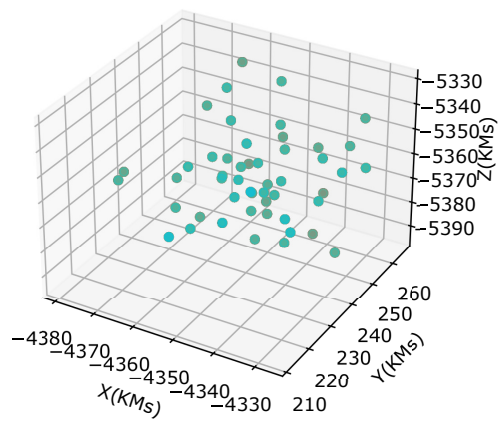


(d) ESPT samples at timestamp = 2701s

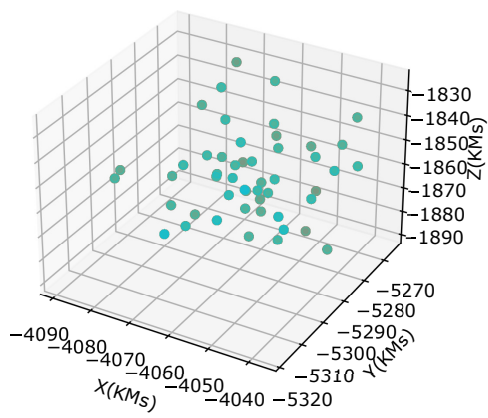
FIGURE 4.8: ESPT samples at timestamp = 1s, 901s, 1801s, 2701s.



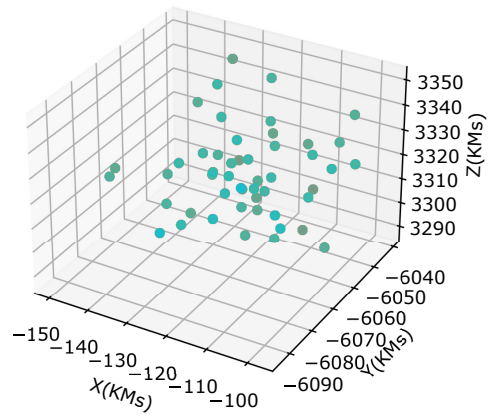
(a) ESPT samples at timestamp = 3601s



(b) ESPT samples at timestamp = 4501s



(c) ESPT samples at timestamp = 5401s



(d) ESPT samples at timestamp = 6301s

FIGURE 4.9: ESPT samples at timestamp = 3601s, 4501s, 5401s, 6301s.

### 4.4.2 Monte Carlo Samples

Sample points of orbit object are propagated to a set of times in the future using the Monte Carlo Method. Here all the samples is propagated to every second until the propagation is completed for 7200s. The samples position is determined after every 900s and a plot is generated.

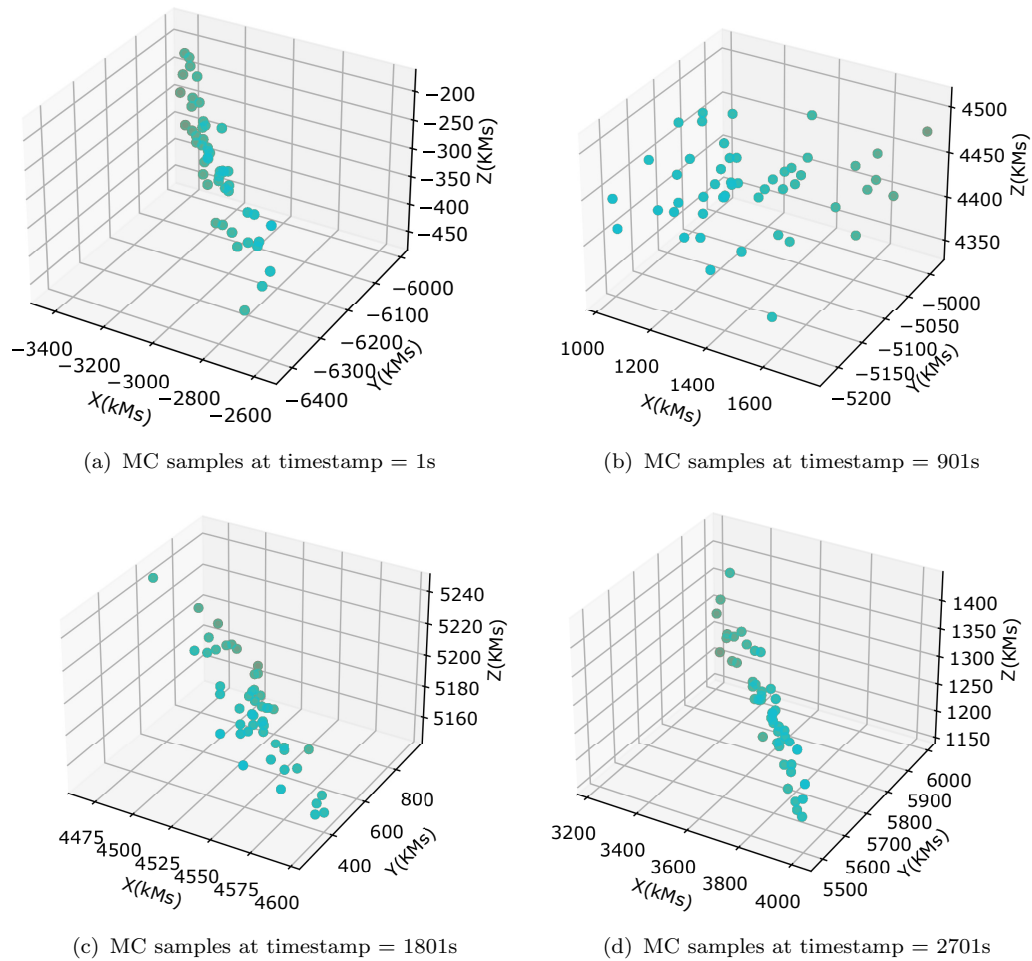
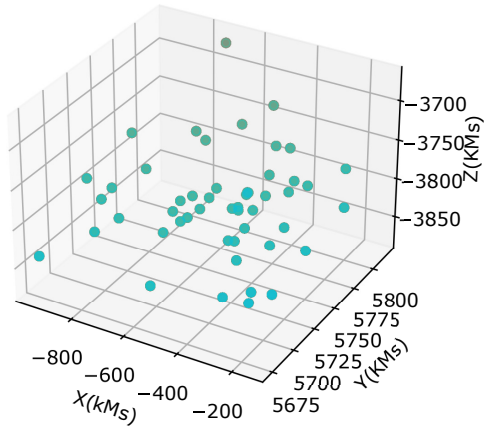
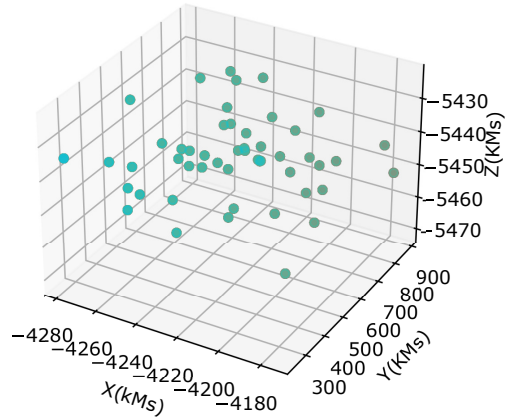


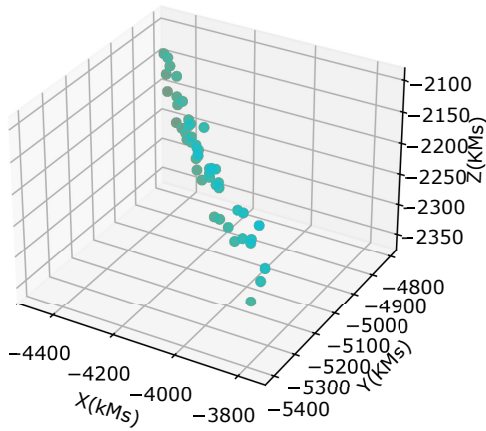
FIGURE 4.10: MC samples at timestamp = 1s, 901s, 1801s, 2701s.



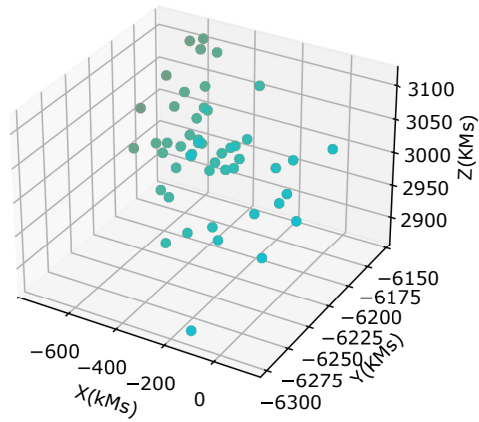
(a) MC samples at timestamp = 3601s



(b) MC samples at timestamp = 4501s



(c) MC samples at timestamp = 5401s



(d) MC samples at timestamp = 6301s

FIGURE 4.11: MC samples at timestamp = 3601s, 4501s, 5401s, 6301s.

## 4.5 Mean and Standard Deviation Plots

While generating the sample points of the orbit object, we considered that the uncertainty associated with the position of the RSO is a Gaussian distribution. Hence it is essential to know the mean and standard deviation of the inter-satellite distance of the samples at each propagating interval. The figures 4.12 - 4.13 and 4.15 - 4.17 shows the mean and standard deviation over time when samples are created using ESPT and the Monte Carlo Method.

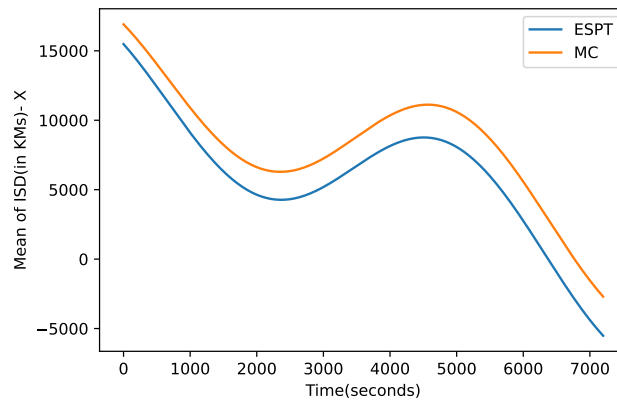


FIGURE 4.12: Plot of Mean of Inter-satellite distance in X axis

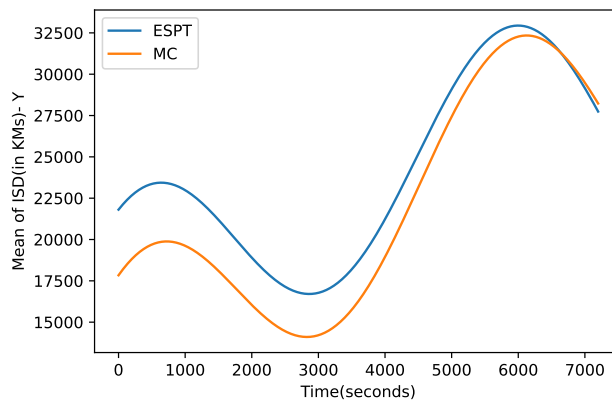


FIGURE 4.13: Plot of Mean of Inter-satellite distance in Y axis

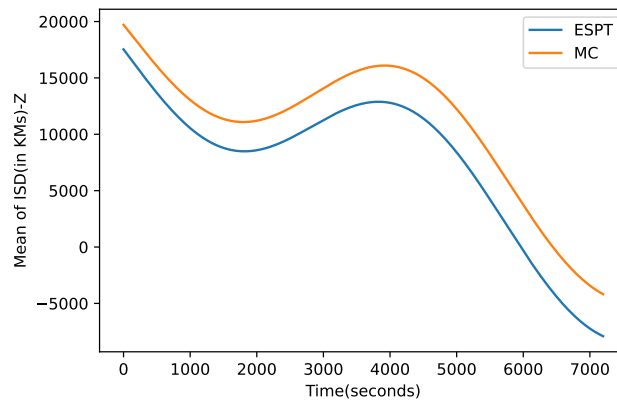


FIGURE 4.14: Plot of Mean of Inter-satellite distance in Z axis

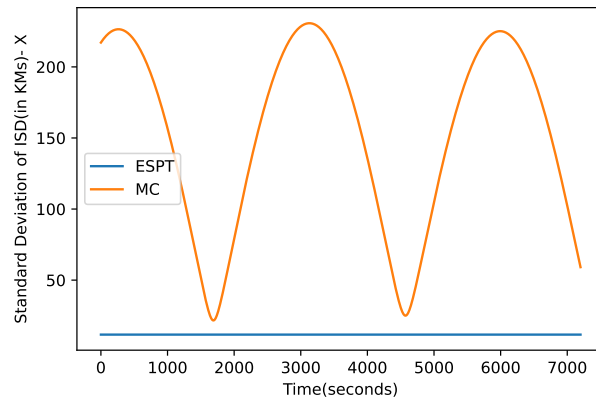


FIGURE 4.15: Plot of Standard deviation of ISD in X

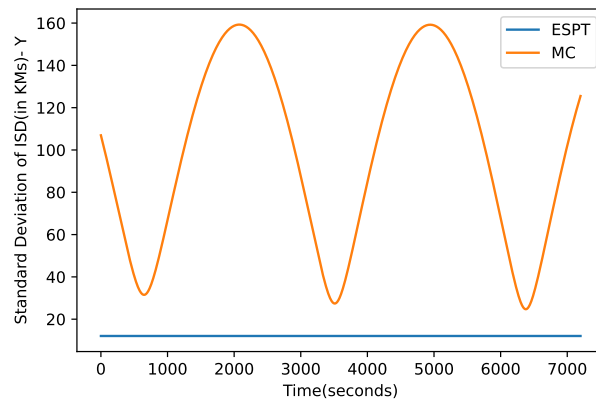


FIGURE 4.16: Plot of Standard deviation of ISD in Y

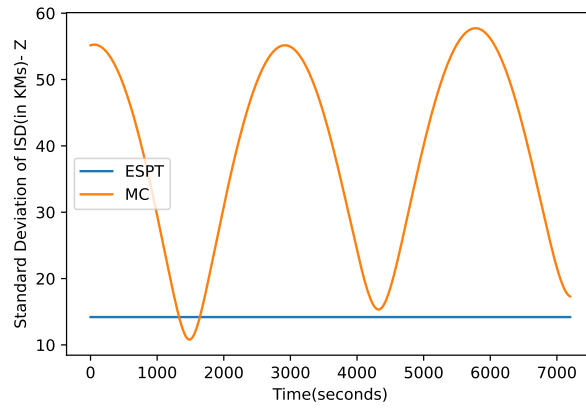


FIGURE 4.17: Plot of Standard deviation of ISD in Z

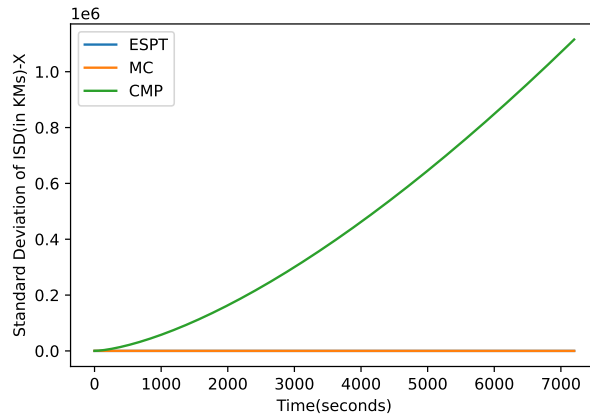


FIGURE 4.18: Plot of Standard deviation of ISD in X from covariance matrix

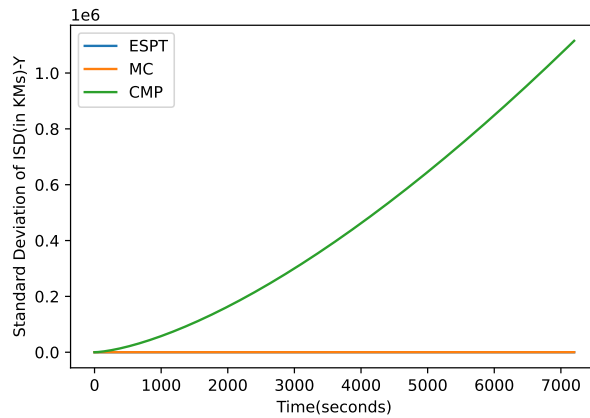


FIGURE 4.19: Plot of Standard deviation of ISD in Y from covariance matrix

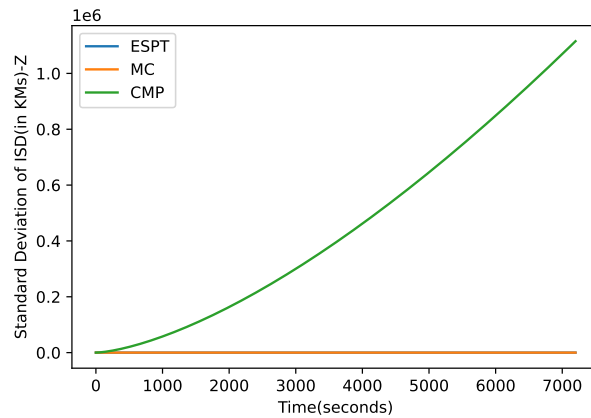


FIGURE 4.20: Plot of Standard deviation of ISD in Z from covariance matrix

Figures 4.20 - 4.19 shows the standard deviation estimated from the covariance matrix for all three methods. It is evident that the standard deviation is increasing exponentially for the CMP method when compared to MC and ESPT methods. Also, the samples generated follow Gaussian distribution, and there is only a slight deviation from the mean in the case of ESPT and MC methods. The results show that these sampling techniques accurately represent the uncertainty associated with the RSOs.

## 4.6 Comparison of Execution Time

For the secondary object with NORAD CAT ID 46137, propagation is done using all three methods, Monte Carlo Method(MC), Extrapolated Single Propagation Technique(ESPT), and Covariance Matrix Propagation Method(CMP), to generate the covariance matrix. The object is propagated for 2 hours in the future, and covariance matrices are generated for each second using all three methods. Table 4.1 shows the comparison of execution times of each method.

Method	Time Taken
MC Method	380 minutes
ESPT Method	117 minutes
CMP Method	15.8 seconds

TABLE 4.1: Comparison of Execution Times of all methods

From the information given in the table, it is clear that ESPT method provides the result much faster than the conventional Monte Carlo method. Even though the covariance propagation method is very much faster than both the methods, after a certain point of time, its standard deviation increases, making it unreliable.

In the ESPT Method, one drawback is observed; propagation can only be done in small intervals of  $\delta t$  up to the time to which we need the result, whereas when the Monte Carlo or CMP method is used, propagation can be done to any time in the future



# Chapter 5

## Conclusion and Future Work

### 5.1 Summary

This work aimed to identify a better and efficient method to estimate the relative distance covariance of resident space objects. Since the number of space objects is very high and increasing exponentially, the analysis is computationally heavy. Each method of covariance estimation, the conventional Monte Carlo (MC) Approach, the direct Covariance Matrix Propagation (CMP) Method and Extrapolated Single Propagation Technique (ESPT) is implemented separately to determine the computational complexity and utility of each method. The Monte Carlo Method turned out to be the slowest and CMP Method turned out to be the fastest Method with regards to computation time. The ESPT Method reduced the computation time to a great extent and also generated results such as miss distance and time of closest approach. Eventhough the CMP method turned out to be the fastest, it was unable to generate the miss distance and time of closest approach. Thus, the ESPT method proved to be most efficient as it reduced the computation time to a great

extend as well as generated crucial results including miss distance and time of closest approach.

## 5.2 Scope for Future Work

In this thesis, we have worked on the determination of the relative distance covariance of resident space objects. This work also includes the determination of miss distance and time of closest approach. The relative distance covariance matrix is crucial because it gives the uncertainty associated with the relative position difference of the space objects.

Due to the huge amount of data present for the space objects, the computation time has been compared for three methods considering only two space objects, and only a small number of samples have been created for each orbit object. To get a much clearer understanding of the uncertainty, the sample numbers have to be scaled up to a huge extent.

A further improvement in the ESPT method can also be made by finding a way to include the higher Taylor series terms while reconstructing the samples. This will model the uncertainty of the space object in a much better way.

The next step in the prevention of a conjunction event is determining the actual probability of collision between two space objects. This can be determined using the estimated relative position covariance matrix. The idea is to create a PDF from the covariance matrix and integrate the PDF with respect to the volume of a warning box around the object. Determining the collision probability can also pave the way to compare the methods based on their accuracy.

---

# References

- [1] John A Kennewell and Ba-Ngu Vo. An Overview of Space Situational Awareness. page 8.
- [2] Howard D. Curtis. *Orbital mechanics for engineering students*. Elsevier Aerospace engineering series. Elsevier Butterworth Heinemann, Amsterdam Heidelberg, 1. ed., reprinted edition, 2008. ISBN 978-0-7506-6169-0.
- [3] A K Anilkumar and D Sudheer Reddy. STATISTICAL CONJUNCTION ANALYSIS OF LEO SPACE OBJECTS: A MONTE CARLO APPROACH. page 6.
- [4] Abdul Rachman and Tiar Dani. Generating two-line elements (TLE) of artificial space objects from optical observations: Preliminary results. *AIP Conference Proceedings*, 1677(1):050013, September 2015. ISSN 0094-243X. doi: 10.1063/1.4930674. URL <https://aip.scitation.org/doi/abs/10.1063/1.4930674>. Publisher: American Institute of Physics.
- [5] J. Šilha. Small telescopes and their application in space debris research and space surveillance tracking. *Contributions of the Astronomical Observatory Skalnaté Pleso*, 49:307–319, May 2019. ISSN 0583-466X. URL <http://adsabs.harvard.edu/abs/2019CoSka..49..307S>.

- 
- [6] George Veis. Optical tracking of artificial satellites. *Space Science Reviews*, 2(2):250–296, August 1963. ISSN 1572-9672. doi: 10.1007/BF00216781. URL <https://doi.org/10.1007/BF00216781>.
- [7] Ju-Hyeon Hong, Jeong-Hun Kim, Seonggyun Kim, and Chang-Kyung Ryoo. TLE data based precise estimation of satellite’s orbital parameters. In *2016 16th International Conference on Control, Automation and Systems (ICCAS)*, pages 1025–1030, October 2016. doi: 10.1109/ICCAS.2016.7832435.
- [8] Sriram Krishnaswamy and Mrinal Kumar. A Window-based Tensor Decomposition Approach to Data-Association for Multi Target Tracking. In *2019 American Control Conference (ACC)*, pages 5148–5153, July 2019. doi: 10.23919/ACC.2019.8815143. ISSN: 2378-5861.
- [9] Alessandro Morselli, Roberto Armellin, Pierluigi Di Lizia, and Franco Bernelli Zazzera. A high order method for orbital conjunctions analysis: Monte Carlo collision probability computation. *Advances in Space Research*, 55(1): 311–333, January 2015. ISSN 02731177. doi: 10.1016/j.asr.2014.09.003. URL <https://linkinghub.elsevier.com/retrieve/pii/S0273117714005675>.
- [10] Li Bin, Jizhang Sang, and Jinsheng Ning. A multiscaling-based semi-analytic orbit propagation method for the catalogue maintenance of space debris. *Journal of Spatial Science*, 65:1–23, July 2018. doi: 10.1080/14498596.2018.1488630.
- [11] Xiao-Li Xu and Yong-Qing Xiong. A method for calculating probability of collision between space objects. *Research in Astronomy and Astrophysics*, 14(5): 601–609, May 2014. ISSN 1674-4527. doi: 10.1088/1674-4527/14/5/009. URL <https://iopscience.iop.org/article/10.1088/1674-4527/14/5/009>.
- [12] Satyendra Singh. A new tool for conjunction analysis of ISRO’s operational satellites, Close Approach Prediction Software: CLAPS. *Journal of Space Safety*

- Engineering*, 7(3):290–294, September 2020. ISSN 2468-8967. doi: 10.1016/j.jsse.2020.06.008. URL <https://www.sciencedirect.com/science/article/pii/S2468896720300598>.
- [13] G. Tommei, A. Milani, and A. Rossi. Orbit determination of space debris: admissible regions. *Celestial Mechanics and Dynamical Astronomy*, 97(4):289–304, April 2007. ISSN 1572-9478. doi: 10.1007/s10569-007-9065-x. URL <https://doi.org/10.1007/s10569-007-9065-x>.
- [14] Ho-Nien Shou. Orbit Propagation and Determination of Low Earth Orbit Satellites. *International Journal of Antennas and Propagation*, 2014:1–12, 2014. ISSN 1687-5869, 1687-5877. doi: 10.1155/2014/903026. URL <http://www.hindawi.com/journals/ijap/2014/903026/>.
- [15] Rahman Hussain Salih. ATMOSPHERIC DRAG PERTURBATION EFFECT ON THE SATELLITES ORBITS. page 11, 2008.
- [16] Matteo Romano, Matteo Losacco, Camilla Colombo, and Pierluigi Di Lizia. Impact probability computation of near-Earth objects using Monte Carlo line sampling and subset simulation. *Celestial Mechanics and Dynamical Astronomy*, 132(8):42, August 2020. ISSN 1572-9478. doi: 10.1007/s10569-020-09981-5. URL <https://doi.org/10.1007/s10569-020-09981-5>.
- [17] Joseph N. Pelton and Scott Madry, editors. *Handbook of Small Satellites: Technology, Design, Manufacture, Applications, Economics and Regulation*. Springer International Publishing, Cham, 2020. ISBN 978-3-030-36307-9 978-3-030-36308-6. doi: 10.1007/978-3-030-36308-6. URL <https://link.springer.com/10.1007/978-3-030-36308-6>.
- [18] Thomas Uriot, Dario Izzo, Luís F. Simões, Rasit Abay, Nils Einecke, Sven Rehan, Jose Martinez-Heras, Francesca Letizia, Jan Siminski, and Klaus Merz.

- Spacecraft collision avoidance challenge: Design and results of a machine learning competition. *Astrodynamics*, 6(2):121–140, June 2022. ISSN 2522-008X, 2522-0098. doi: 10.1007/s42064-021-0101-5. URL <https://link.springer.com/10.1007/s42064-021-0101-5>.
- [19] Sanat K. Biswas and Andrew G. Dempster. Approximating Sample State Vectors Using the ESPT for Computationally Efficient Particle Filtering. *IEEE Transactions on Signal Processing*, 67(7):1918–1928, April 2019. ISSN 1941-0476. doi: 10.1109/TSP.2019.2897955. Conference Name: IEEE Transactions on Signal Processing.
- [20] Shubhi Singhal. SPACE SITUATIONAL AWARENESS. Technical report, 2022.